

Field- and Pressure-Induced Phases in $\text{Sr}_4\text{Ru}_3\text{O}_{10}$: A Spectroscopic Investigation

Rajeev Gupta,¹ M. Kim,¹ H. Barath,¹ S. L. Cooper,¹ and G. Cao²

¹*Department of Physics and Frederick Seitz Materials Research Laboratory, University of Illinois, Urbana, Illinois 61801, USA*

²*Department of Physics, University of Kentucky, Lexington, Kentucky 40506, USA*

(Received 2 August 2005; published 15 February 2006)

We have investigated the magnetic-field- and pressure-induced structural and magnetic phases of the triple-layer ruthenate $\text{Sr}_4\text{Ru}_3\text{O}_{10}$. Magnetic-field-induced changes in the phonon spectra reveal dramatic spin-reorientation transitions and strong magnetoelastic coupling in this material. Further, we are able to deduce key magnetoelastic coupling parameters, and evidence that the magnetic moments are localized on the Ru sites. Additionally, pressure-dependent Raman measurements at different temperatures reveal an anomalous negative Gruneisen parameter associated with the B_{1g} mode ($\sim 380 \text{ cm}^{-1}$) at low temperatures ($T < 75 \text{ K}$), which can be explained consistently with the field-dependent Raman data.

DOI: 10.1103/PhysRevLett.96.067004

PACS numbers: 74.70.Pq, 75.25.+z, 78.30.-j

Spin-lattice coupling plays a critical role in the exotic properties and phases exhibited by a variety of oxide-based materials having both geometrical and chemical complexity; these include geometrically frustrated magnets such as ZnCr_2O_4 [1], low-dimensional spin systems such as $(\text{TMTSF})_2\text{PF}_6$ and CuGeO_3 [2], hexagonal multiferroic manganites [3], and layered ruthenates [4]. The large spin-phonon coupling in these materials leads not only to remarkable phenomena—such as magnetoferroelectricity, magnetic-field-induced metal-insulator transitions, and “colossal” magnetoelastic effects—but also to highly tunable phase behavior in which structural properties can be sensitively manipulated by an applied magnetic field, or conversely in which magnetic properties can be controlled with applied pressure or strain.

The Sr-based layered ruthenates, such as double-layer $\text{Sr}_3\text{Ru}_2\text{O}_7$ and triple-layer $\text{Sr}_4\text{Ru}_3\text{O}_{10}$, are particularly interesting materials from the perspective of spin-lattice coupling. For example, $\text{Sr}_3\text{Ru}_2\text{O}_7$ is an enhanced Pauli paramagnet [5,6] that exhibits induced ferromagnetism upon the application of hydrostatic pressure [5] or magnetic field [7,8]. Density functional calculations suggest that the induced ferromagnetism in double-layer $\text{Sr}_3\text{Ru}_2\text{O}_7$ results from rotations of the RuO_6 octahedra, which lead to an orthorhombically distorted unit cell [9]. Furthermore, triple-layer $\text{Sr}_4\text{Ru}_3\text{O}_{10}$ is a structurally distorted (antiferromagnetically) canted ferromagnet with a Curie temperature of $T_C = 105 \text{ K}$, in which the RuO_6 octahedra in the outer 2 RuO layers are rotated 5.25° about the c axis, while the RuO_6 octahedra in the central RuO layer are rotated 10.6° about the c axis in the opposite direction [6]. Hence, one also expects in this system a sensitive coupling between the structural and magnetic properties. For example, Raman measurements of Iliev *et al.* [10] show that the frequency of the 380 cm^{-1} B_{1g} phonon in $\text{Sr}_4\text{Ru}_3\text{O}_{10}$ is highly sensitive to the onset of ferromagnetic order.

In this Letter, we investigate the intimate coupling between the spin and lattice degrees of freedom in $\text{Sr}_4\text{Ru}_3\text{O}_{10}$ using field- and pressure-dependent inelastic light scattering. The strong spin-lattice coupling in the material allows

us to use the frequency of the B_{1g} phonon near 380 cm^{-1} as a means of exploring the spin-spin correlation function as functions of field and pressure. These results provide specific details regarding the strong spin-phonon coupling in $\text{Sr}_4\text{Ru}_3\text{O}_{10}$. For example, we are able to deduce from these results the detailed H - T phase diagrams, the spin-phonon coupling parameter, and the specific magnetoelastic mechanism for the metamagnetic transition below $T < 50 \text{ K}$ [11,12] in $\text{Sr}_4\text{Ru}_3\text{O}_{10}$.

Our measurements were carried out on well-characterized single crystals ($1 \times 1 \times 0.5 \text{ mm}^3$) of $\text{Sr}_4\text{Ru}_3\text{O}_{10}$, which were grown by flux techniques [11]. Transport and magnetization results on these samples are consistent with those in other published reports [6,11]. The high purity and quality of the $\text{Sr}_4\text{Ru}_3\text{O}_{10}$ crystals studied here are clearly demonstrated by the observation of quantum oscillations [11], as well as by the fact that these samples have a Dingle temperature that is less than 3 K, which is comparable to values found in high-quality organic crystals (0.5 to 3.5 K). Field-dependent Raman measurements were performed in both Faraday ($H \parallel c \text{ axis} \parallel \vec{k}$) and Voigt ($H \parallel ab \text{ plane} \perp \vec{k}$) configurations [4], and high-pressure Raman measurements were performed using a moissanite anvil cell [13].

Magnetization [6,11] and x-ray diffraction measurements [6] reveal that $\text{Sr}_4\text{Ru}_3\text{O}_{10}$ is a canted ferromagnet below $T_C = 105 \text{ K}$, with the Ru moments oriented primarily along the c axis, as shown in Fig. 1(c). Notably, Fig. 1 shows that the temperature dependence of the B_{1g} phonon frequency—which is associated with internal vibrations of the RuO_6 octahedra [10]—exhibits a distinct change in slope, $d\omega/dT$, below T_C , as observed previously [10]. This anomalous frequency dependence is indicative of a strong magnetoelastic coupling between the B_{1g} phonon mode and the c axis ordered Ru-moments.

Upon the application of a magnetic field along the c axis direction, the B_{1g} phonon frequency exhibits a frequency increase with field, which has its largest value ($\sim 3 \text{ cm}^{-1}$) for $T \ll T_C$. This field-induced phonon frequency shift

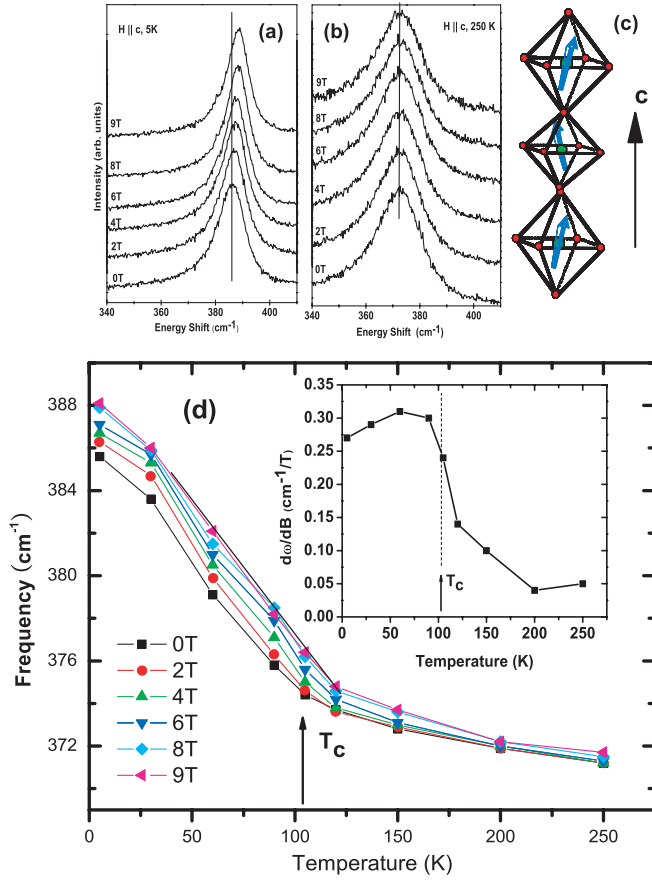


FIG. 1 (color). Representative Raman spectra of the B_{1g} phonon mode in $\text{Sr}_4\text{Ru}_3\text{O}_{10}$ as a function of magnetic field with $H \parallel c$ axis for (a) $T = 5$ K and (b) $T = 250$ K. (c) Picture of the orientation of the Ru moments in the FM phase in the three layers of octahedral RuO_6 . (d) Temperature dependence of the phonon frequency (ω) at different magnetic fields. The inset shows the slope $d\omega/dB$ as a function of temperature.

below T_C indicates that an applied field parallel to the c axis reduces the canting of the moments by causing the RuO_6 octahedra to increase their elongation along the c axis, resulting in a contraction of the in-plane RuO bonds and a corresponding increase in the frequency of the in-plane B_{1g} vibrational mode. This result identifies a specific structural mechanism associated with the weakly field-dependent c axis magnetization in $\text{Sr}_4\text{Ru}_3\text{O}_{10}$ [6,11].

One can examine more quantitatively the magnetoelastic coupling between the RuO phonon and the Ru spins in the ferromagnetic (FM) phase by noting that the contribution of spin-spin correlations to the phonon frequency can be approximated as [14,15] $\omega = \omega_0 + \lambda \langle \mathbf{S}_i \cdot \mathbf{S}_j \rangle$, where ω_0 is the bare phonon frequency in the absence of spin-phonon interactions, λ is the spin-phonon coupling parameter, and \mathbf{S}_i is the spin on the i th Ru site. In $\text{Sr}_4\text{Ru}_3\text{O}_{10}$, the magnetic interactions are FM along the c axis direction, and weak-antiferromagnetic (AFM) or paramagnetic (PM) in the ab plane. One can therefore approximate the spin-spin correlation function—within a molecu-

lar field approximation—by treating $\text{Sr}_4\text{Ru}_3\text{O}_{10}$ as a FM chain along the c direction and taking an ensemble average over nearest-neighbor sites [16]: $\langle \mathbf{S}_i \cdot \mathbf{S}_j \rangle \approx 2[M/2\mu_B]^2$. This relation assumes a saturation moment of 2 for the $S = 1$ spin state of Ru. The resulting expression for the field dependence of the magnetoelastic phonon frequency can be written:

$$\frac{\partial \omega}{\partial B} = 2\pi\lambda \left(\frac{M}{\mu_B^2} \right) \frac{\partial M}{\partial B}. \quad (1)$$

Putting the measured values of $\frac{\partial \omega}{\partial B} = 0.27 \text{ cm}^{-1}/\text{T}$ (at 5 K) and $\frac{\partial M}{\partial B} = 0.0083 \mu_B/\text{T}$ [at 1.7 K [11]] in Eq. (1), we estimate the magnitude of the spin-phonon coupling constant for the B_{1g} mode in $\text{Sr}_4\text{Ru}_3\text{O}_{10}$ to be $\lambda = 5.2 \text{ cm}^{-1}$ for $T \ll T_C$; this coupling reflects a strong sensitivity of the exchange interaction to atomic displacements below T_C , and is comparable to values observed in other strong spin-lattice coupled systems such as ZnCr_2O_4 [1].

It is also of interest to examine the magnetoelastic effects of applying a magnetic field in the ab plane direction. Previous magnetization measurements [11] with $H \parallel ab$ plane have identified a metamagnetic transition above $H_c \sim 2$ T for temperatures $T < 50$ K, although the specific nature of this transition has not yet been identified. Adding further interest to this transition, recent transport measurements of $\text{Sr}_4\text{Ru}_3\text{O}_{10}$ have identified abrupt resistive jumps in this field-induced transition, indicative of some form of switching behavior [12]. In order to better identify the specific nature of this interesting field-induced transition, as well as the significance of the temperature scale T^* below which this transition is observed, we show in Fig. 2 the field-dependent Raman spectra of $\text{Sr}_4\text{Ru}_3\text{O}_{10}$ at various fixed temperatures for $H \parallel ab$ plane. Interestingly, Fig. 2 shows that there is little change in the B_{1g} phonon frequency with increasing field for temperatures $50 \text{ K} < T < T_C$. However, for $T < 50$ K, the B_{1g} phonon frequency exhibits a significant decrease with increasing field up to a critical field $H < H_c = 2$ T, above which little or no additional change in the frequency is observed with field. These results demonstrate a distinct structural contribution to the metamagnetic transition near $H_c \sim 2$ T, in which an applied field induces the Ru moments away from the c axis, increasing the in-plane RuO bonds in the RuO_6 octahedra, and decreasing the B_{1g} phonon frequency. This implies that the metamagnetic transition for $T < T^* \sim 50$ K and $H_c \sim 2$ T is associated with a transition from an AFM or PM canted arrangement of the Ru moments to a FM canted arrangement [see Fig. 3(a)]. This result further suggests that the “switching” behavior observed in transport measurements [12] through this field-induced transition is actually associated with inhomogeneous flipping of large regions of the sample from an AFM/PM canting arrangement to a FM canting arrangement. The change from AFM/PM to FM canting most likely influences the in-plane conductivity by reduc-

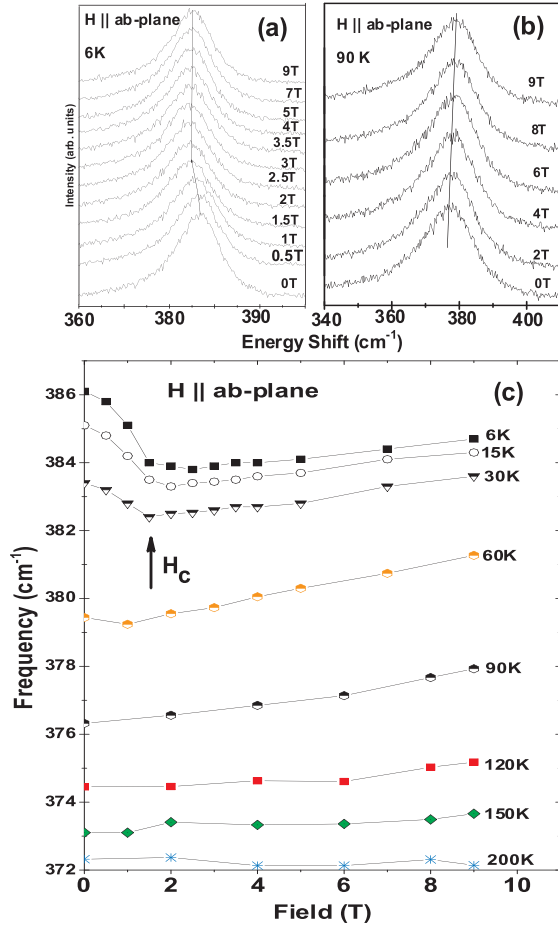


FIG. 2 (color). Raman spectra of the B_{1g} phonon mode in $\text{Sr}_4\text{Ru}_3\text{O}_{10}$ as a function of magnetic field for $H \parallel ab$ plane for (a) $T = 6$ K and (b) $T = 90$ K. (c) Field dependence of the B_{1g} phonon frequency for different temperatures. Possible laser heating effects of about ~ 5 K have not been included in the temperatures shown.

ing in-plane spin scattering. Note also that the strong magnetoelastic coupling evident in this material, which enables us to manipulate the structural properties with an applied magnetic field, suggests that the magnetic moments are localized on the Ru sites.

This interpretation of the metamagnetic transition in $\text{Sr}_4\text{Ru}_3\text{O}_{10}$ raises questions about the nature of the temperature scale $T^* \sim 50$ K below which the metamagnetic transition is observed. We suggest that in the temperature range $T^* < T < T_C$, the Ru moments are canted and FM aligned along the c direction, but that there is no ordering of the in-plane component of the moments in the ab plane. For temperatures below $T^* = 50$ K, however, the moments “lock” into an AFM canted or a PM configuration for $H < H_c = 2$ T, and into a FM canted configuration for $H > H_c$. We summarize the rich field-temperature phase diagram of $\text{Sr}_4\text{Ru}_3\text{O}_{10}$ for $H \parallel ab$ plane in Fig. 3(a). Of particular interest in this phase diagram are the following features: at low temperatures ($T < 50$ K), the system undergoes a

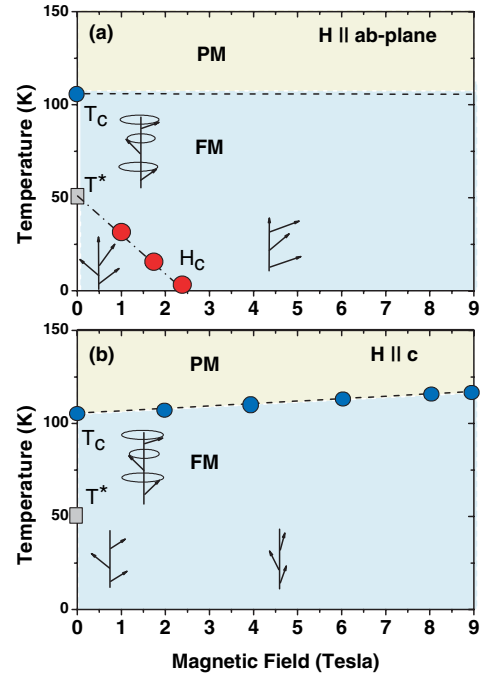


FIG. 3 (color). (a) Proposed (H, T) phase diagram for $\text{Sr}_4\text{Ru}_3\text{O}_{10}$ for $H \parallel ab$ plane, as deduced from the field-dependent phonon data. Red dots show the dependence of H_c on temperature taken from magnetization measurements of Ref. [11]. (b) Proposed (H, T) phase diagram for $\text{Sr}_4\text{Ru}_3\text{O}_{10}$ for $H \parallel c$ axis.

metamagnetic transition from an AFM or PM canted configuration of the Ru moments to a FM canted configuration above $H_c \sim 2$ T. We also show the variation of H_c as a function of the in-plane applied field at different temperatures, which was obtained from isothermal magnetization measurements [11]. In the temperature range $50 \text{ K} < T < T_C$, the Ru moments are FM aligned along the c axis direction, but there is no net in-plane ordering for in-plane fields within our field range. For $T > T_C$, the Ru moments are randomly oriented in all directions. For comparison, the simpler field-temperature phase diagram of $\text{Sr}_4\text{Ru}_3\text{O}_{10}$ for $H \parallel c$ axis is shown in Fig. 3(b). The key feature of this phase diagram is a FM transition temperature that increases slightly from 105 K at 0 T to ~ 115 K at 9 T.

Given its strong magnetoelastic coupling, it is also of interest to investigate the extent to which one can influence the magnetic properties of $\text{Sr}_4\text{Ru}_3\text{O}_{10}$ at high pressures. Figure 4 summarizes the B_{1g} phonon frequency as a function of temperature at various (quasihydrostatic) pressures, while the inset of Fig. 4 summarizes the derivative of the B_{1g} mode frequency with respect to pressure, $d\omega/dP$, at various temperatures. Note that $d\omega/dP$ is related to the mode Grüneisen parameter, defined as $\gamma_i = \frac{1}{\omega_i \chi_T} \frac{d\omega_i}{dP}$, where ω_i is the frequency of the i th mode, P is the pressure, and χ_T is the isothermal compressibility. Below $T \sim 70$ K, there is a large decrease in the B_{1g}

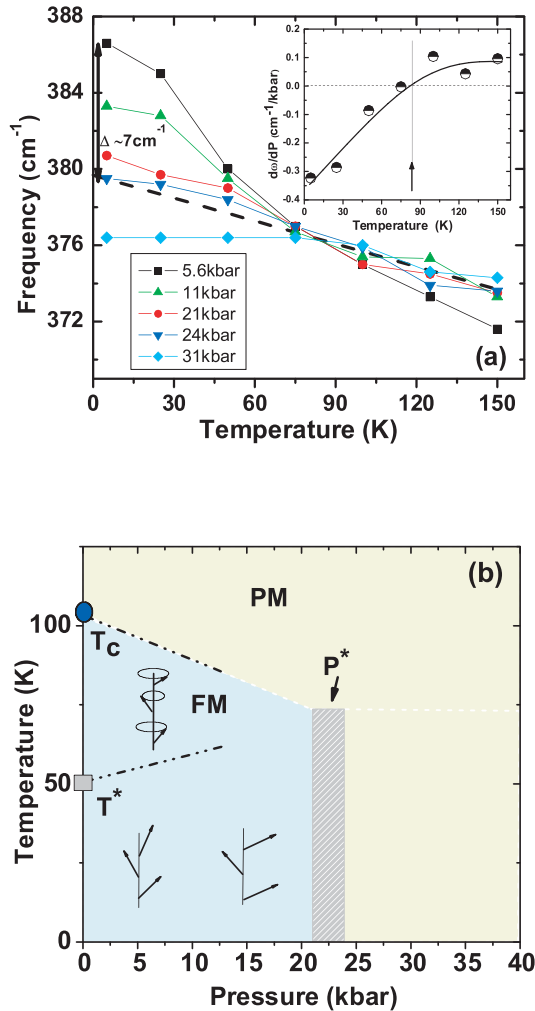


FIG. 4 (color). (a) Temperature dependence of the B_{1g} phonon mode for different pressures. The inset shows the pressure derivative of the phonon frequency as a function of temperature, and the vertical line indicates the temperature (~ 75 K) below which $d\omega/dP$ has a negative value. (b) Proposed (P, T) phase diagram, for isobaric paths, for $\text{Sr}_4\text{Ru}_3\text{O}_{10}$, as deduced from the pressure-dependent phonon data.

phonon frequency with increasing pressure: $d\omega/dP = -0.32 \text{ cm}^{-1}/\text{kbar}$ at $T = 5$ K. This is associated with the pressure-induced buckling of the RuO_6 octahedra on adjacent RuO layers, which forces the Ru moments to cant toward the ab plane with increasing pressure, in opposition to the tendency for c axis FM ordering at $P = 0$. Consequently, the pressure-induced frequency shift of the B_{1g} mode provides a measure of the magnetoelastic energy stored by the Ru moments and the RuO_6 octahedra in the FM phase. Interestingly, Fig. 4(a) shows that for $P \sim 24$ kbar, the B_{1g} phonon frequency has a roughly linear temperature dependence, with no anomalous change in slope through T_C , suggesting that the pressure-induced buckling of the RuO_6 octahedra on adjacent RuO layers at this pressure completely suppresses c axis ferromagne-

tism for isobaric temperature sweeps, presumably by suppressing the RuO_6 rotations that accompany c axis FM ordering in $\text{Sr}_4\text{Ru}_3\text{O}_{10}$. This conclusion supports the observation that the phonon frequency reduction between $P = 0$ and $P = 24$ kbar is $\Delta \sim 7 \text{ cm}^{-1}$ at $T = 5$ K, which is comparable to the magnetoelastic energy estimated from the magnetic field-dependent measurements. Based upon these results, we infer the (P, T) phase diagram for $\text{Sr}_4\text{Ru}_3\text{O}_{10}$ shown in Fig. 4(b). Our results suggest that high-pressure magnetization measurements will exhibit a suppression of the c axis magnetic moment for $T < T_C$, as pressure causes increased canting of the Ru moments away from the c axis direction. Further, Fig. 4(b) shows that T_C decreases with increasing pressure, culminating in the absence of c axis ferromagnetism (for isobaric temperature sweeps) above $P^* \sim 24$ kbar, and that the “lock-in” temperature T^* increases with pressure.

In summary, we have used field- and pressure-dependent Raman spectroscopy to explore the strong spin-lattice coupling in $\text{Sr}_4\text{Ru}_3\text{O}_{10}$, and to provide a comprehensive microscopic description of the structural and magnetic (H, T) and (P, T) phases for this material. In addition to a large spin-phonon coupling parameter $\lambda \sim 5.2 \text{ cm}^{-1}$, we find evidence for a field-induced change from an AFM or PM canted arrangement of the Ru moments to a FM canted arrangement for $H_c > 2$ T ($H \parallel ab$ plane) and a suppression of the c axis aligned FM phase for pressures above roughly 24 kbar. The strong magnetoelastic coupling in $\text{Sr}_4\text{Ru}_3\text{O}_{10}$ provides strong evidence that the magnetic moments are localized on the Ru sites.

We acknowledge support by the National Science Foundation under Grants No. DMR02-44502 (S.L.C.) and No. DMR02-40813 (G.C.), and the Department of Energy under Grant No. DEFG02-91ER45439 (S.L.C.).

- [1] A. B. Sushkov *et al.*, Phys. Rev. Lett. **94**, 137202 (2005).
- [2] M. Lang *et al.*, J. Phys. IV **114**, 111 (2004).
- [3] T. Kimura *et al.*, Nature (London) **426**, 55 (2003).
- [4] J. F. Karpus *et al.*, Phys. Rev. Lett. **93**, 167205 (2004).
- [5] S. I. Ikeda *et al.*, Phys. Rev. B **62**, R6089 (2000).
- [6] M. K. Crawford *et al.*, Phys. Rev. B **65**, 214412 (2002).
- [7] R. S. Perry *et al.*, Phys. Rev. Lett. **86**, 2661 (2001).
- [8] S. A. Grigera *et al.*, Science **294**, 329 (2001).
- [9] D. J. Singh and I. I. Mazin, Phys. Rev. B **63**, 165101 (2001).
- [10] M. N. Iliev *et al.*, Physica (Amsterdam) **358B**, 138 (2005).
- [11] G. Cao *et al.*, Phys. Rev. B **68**, 174409 (2003).
- [12] Z. Mao *et al.*, cond-mat/0406439.
- [13] C. S. Snow *et al.*, Phys. Rev. Lett. **89**, 226401 (2002).
- [14] D. J. Lockwood and M. G. Cottam, J. Appl. Phys. **64**, 5876 (1988).
- [15] X. K. Chen, J. C. Irwin, and J. P. Franck, Phys. Rev. B **52**, R13130 (1995).
- [16] A. H. Morrish, *Physical Principles of Magnetism* (Wiley, New York, 1965).